INTERNATIONAL JOURNAL FOR NUMERICAL METHODS IN FLUIDS, VOL. 23, 923–936 (1996)

MULTIDIMENSIONAL UPWIND RESIDUAL DISTRIBUTION SCHEMES FOR THE CONVECTION–DIFFUSION EQUATION

H. PAILLÈRE,* J. BOXHO, G. DEGREZ AND H. DECONINCK

Von Karman Institute for Fluid Dynamics, Chaussée de Waterloo 72, B-1640 Rhode St-Genèse, Belgium

SUMMARY

Multidimensional residual distribution schemes for the convection–diffusion equation are described. Compact upwind cell vertex schemes are used for the discretization of the convective term. For the diffusive term, two approaches are compared: the classical finite element Galerkin formulation, which preserves the compactness of the stencil used for the convective part, and various residual-based approaches in which the diffusive term, evaluated after a reconstruction step, is upwinded along with the convective term.

KEY WORDS: advection–diffusion; multidimensional upwinding; finite elements

1. INTRODUCTION

The scalar convection–diffusion equation with constant convection speed and viscosity represents a simple scalar model for the Navier–Stokes equations of fluid flow. It incorporates both a convection term $\vec{\lambda} \cdot \nabla u$ and a diffusion term $\nu \Delta u$ which models viscous effects:

$$\frac{\partial u}{\partial t} + \vec{\lambda} \cdot \nabla u = \nu \Delta u. \tag{1}$$

Introducing the non-dimensional cell Peclet number Pe representing the ratio of convection effects over diffusion effects and defined as $Pe = \lambda h / \nu$, where h is a characteristic length of the space discretization, three regimes can be distinguished:

(a) $Pe \leqslant 1$ where the flow is diffusion-dominated
(b) $1 < Pe \leqslant 10$ where convection and diffusion effects are both important
(c) $Pe > 10$ where the flow is convection-dominated.

$Pe = 0$ corresponds to pure diffusion and $Pe = \infty$ corresponds to pure convection. The Peclet number plays the same role as the Reynolds number in fluid flows. Classically, in the finite volume framework and for $Pe > 1$, upwind differences are preferred for the discretization of the convective part of the equation and central differences are preferred for the diffusive terms. On unstructured meshes the latter is equivalent to the Galerkin finite element method and yields very accurate results for diffusion-dominated (low-Peclet-number) flows. In the cell vertex finite volume method of Morton *et al.*[1] the viscous flux balance is evaluated per cell and distributed along with the inviscid

* Current address: CEA/DMT/SEMT, Laboratoire de Transferts Thermiques et Mécanique des Fluides, F-91191 Gif-sur-Yvette Cedex, France.

CCC 0271–2091/96/090923–14

Received August 1995
Revised February 1996

flux balance using a Lax–Wendroff-type scheme, an approach which the authors claim to be more accurate than the Galerkin method and which is consistent with the residual distribution philosophy.

In this paper both approaches are investigated in the framework of residual distribution schemes using linear triangular elements.[2] The following discretizations are compared.

1. *Mixed upwind/central discretization.* The convective term is discretized using a linearity-preserving convection scheme and the diffusive term is discretized using the Galerkin finite element method. This has the advantages of being inexpensive and, most importantly, of keeping the stencil compact.[3]
2. *Residual-based discretization.* The diffusive term is treated as a source term and distributed with coefficients based on the convective term.[4] This requires an extension of the stencil in order to recover the gradients at the nodes or on the edges of the cells and compute the balance of the viscous fluxes by integration.

2. UPWIND RESIDUAL DISTRIBUTION SCHEMES FOR THE INHOMOGENEOUS CONVECTION EQUATION

Upwind residual distribution schemes on compact stencils for the inhomogeneous convection equation are considered:

$$\frac{\partial u}{\partial t} + \vec{\lambda} \cdot \nabla u + S = 0. \tag{2}$$

These schemes, described in detail in References 2 and 5–8, are based on a continuous, piecewise linear (P1 finite element) representation of the solution on unstructured triangular meshes and use the same compact stencil as the Galerkin finite element method, which offers a number of valuable advantages in terms of computational cost, suitability for implicit iterative strategies and parallel implementation. The residual of 'fluctuation' ϕ_T is obtained by integrating this equation over a triangular cell T:

$$\phi^T = \int\int_T \vec{\lambda} \cdot \nabla u \, \mathrm{d}\Omega + \int\int_T S(x, y) \, \mathrm{d}\Omega = \phi^C + \phi^S. \tag{3}$$

In the residual distribution approach, fractions of ϕ^T are distributed to the vertices of the cell, with scalar coefficients β_i^T summing up to unity for consistency. After assembling contributions from all the cells, each nodal value can be updated as

$$u_i^{n+1} = u_i^n - \frac{\Delta t}{S_i} \sum_T \beta_i^T \phi^T, \tag{4}$$

where S_i represents the area of the median dual cell around node i. Both linear and non-linear upwind distribution schemes on unstructured triangular meshes have been developed over the past years, with built-in properties such as positivity ($\mathscr{P}$) and linearity preservation ($\mathscr{LP}$). The latter property can be defined as

$$\beta_i^T \phi^T \to 0 \quad \text{when } \phi^T = \phi^C + \phi^S \to 0. \tag{5}$$

In other words, the distribution coefficients must remain bounded. It has been shown[8] that on a regular mesh this implies the absence of cross-flow diffusion and hence second-order accuracy at steady state for the homogenous advection equation. Positivity, which guarantees that no spurious

oscillations are created, can be proved in the homogeneous case ($\phi^S = 0$). Assuming constant convection speed $\vec{\lambda}$ and linear variation in u over a triangular cell, the convective residual ϕ^C may be expressed as

$$\phi^C = S_T \vec{\lambda} \cdot \nabla u = k_i u_i^n + k_j u_j^n + k_k u_k^n, \tag{6}$$

where S_T is the area of the cell and k_i is called the inflow parameter, defined as $k_i = \frac{1}{2}\vec{\lambda} \cdot \vec{n}_i$, $\vec{n}_i$ being the inward normal opposite node i and scaled by the length of the edge; see Figure 1. One has $\vec{n}_i + \vec{n}_j + \vec{n}_k = \vec{0}$ and consequently $k_i + k_j + k_k = 0$. Using this notation, the updated scheme can be rewritten as

$$u_i^{n+1} = \sum_l c_l u_l^n, \tag{7}$$

with $\sum c_l = 1$ for consistency. A scheme is said to be positive if all the coefficient c_l are positive. It has been shown that only non-linear schemes can combine the properties of positivity and linearity preservation. Finally, an upwind distribution scheme (U) is such that

$$\beta_i^T = 0 \quad \text{when } k_i < 0. \tag{8}$$

Since the k_l sum up to zero, one has to consider only two cases, depicted in Figure 2: the one-targeted case ($k_i > 0$, $k_j < 0$ and $k_k < 0$) in which the whole residual is distributed to node i and the two-target case ($k_i > 0$, $k_j > 0$ and $k_k < 0$) in which the residual is split between the two downstream nodes i and j. Examples of distribution schemes, including the non-linear positive streamwise invariant (PSI) scheme[2,6] and the shock-capturing streamline upwind Petrov–Galerkin (SUPG) or streamline diffusion scheme,[5,9] are given in Table I

In the presence of a source term the PSI scheme can be extended in the following manner. In the one-target case the whole residual ($\phi^C + \phi^S$) is distributed to the downstream node. In the two-target case the whole residual ($\phi^C + \phi^S$) is distributed to the downstream node. In the two-target case ($k_i > 0$ and $k_j > 0$, provisional updates are determined based on the discretization of ϕ^C using the N scheme and the discretization of ϕ^S using the LDA scheme:

$$\phi_i = k_i(u_i - u_k) - \frac{k_i}{k_k}\phi^S, \qquad \phi_j = k_j(u_j - u_k) - \frac{k_j}{k_k}\phi^S. \tag{9}$$

This scheme is not linearity-preserving, since $\phi^T = 0$ does not imply $\phi_i = \phi_j = 0$. However, applying the MinMod limiter function $L(x, y)$, where $L(x, y) = \frac{1}{2}[1 + \text{sgn}(xy)]\frac{1}{2}[\text{sgn}(x) + \text{sgn}(y)] \times \min(|x|, |y|)$, to ϕ_i and ϕ_j,

$$\phi_i^* = \phi_i - L(\phi_i, -\phi_j), \qquad \phi_j^* = \phi_j - L(\phi_j, -\phi_i), \tag{10}$$

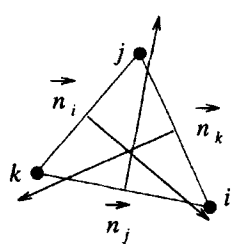

Figure 1. Generic triangle and inward normals $\vec{n}_i$

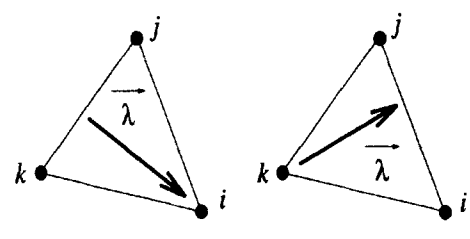

Figure 2. One-target case (left_ and two-target case (right)

Table I. Distribution coefficients β_i for various distribution schemes

Scheme	$\mathscr{U}$	$\mathscr{P}$	$\mathscr{LP}$	Distribution coefficient β_i
Linear				
N (narrow) scheme	√	√		$-\frac{1}{\phi^T}\frac{\max(0,k_i)}{\sum_i \max(0,k_j)}\sum_j \min(0,k_j)(u_i^n - u_j^n)$
Galerkin			√	$\frac{1}{3}$
LDA (low-diffusion A) scheme	√		√	$\frac{\max(0,k_i)}{\sum_j \max(0,k_j)}$
SUPG scheme			√	$\frac{1}{3}+\tau\frac{k_i}{S_T}, \tau=\frac{1}{2}\frac{h}{\|\vec{\lambda}\|}$
Non-linear				
PSI scheme	√	√	√	$\mathrm{MinMod}(\beta_i^N)$
SUPG + AV (artificial viscosity) scheme			√	$\frac{1}{3}+\tau\frac{k_i}{S_T}+\hat{\kappa}\frac{\nabla u\cdot\vec{n}_i}{2S_T\phi^T}, \hat{\kappa}=f(\phi^T)$

one obtains a linearity-preserving scheme, since $\phi_i \to 0$ and $\phi_j \to 0$ when $\phi^T \to 0$, which furthermore reverts to the positive PSI scheme in the absence of a source term.

3. DISCRETIZATIONS FOR THE CONVECTION–DIFFUSION EQUATION

3.1. Mixed upwind/central discretization

In the present approach the convection term is discretized using an upwind (as defined in Section 2) linearity-preserving scheme, while the diffusion term is discretized using a central finite volume formulation of the integral equation on the dual mesh. Considering for instance the median dual cell S_i shown in Figure 3, one has

$$\iint_{S_i} \nu\Delta u \, \mathrm{d}\Omega = \oint_{\partial S_i} \nu\nabla u \cdot \mathrm{d}\vec{n}_{\mathrm{ext}} = \sum_{T\in\Omega_i} \oint_{\partial S_i\cap T} \nu\nabla u \cdot \mathrm{d}\vec{n}_{\mathrm{ext}}. \tag{11}$$

For each triangle T the boundary $\partial S_i \cap T$ is composed of two segments with outward-pointing normals $\vec{n}_{\mathrm{ext}}^1$ and $\vec{n}_{\mathrm{ext}}^2$ such that

$$\vec{n}_{\mathrm{ext}}^1 + \vec{n}_{\mathrm{ext}}^2 = -\frac{1}{2}\vec{n}_i. \tag{12}$$

Substituting into (11), one has

$$\iint_{S_i} \nu\Delta u \, \mathrm{d}\Omega = -\sum_{T\in\Omega_i} \frac{\nu}{2}\nabla u \cdot \vec{n}_i, \tag{13}$$

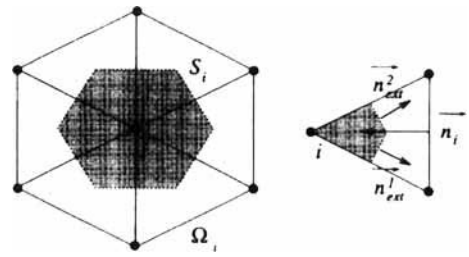

Figure 3. Median dual cell S_i and compact support Ω_i of triangles meeting in i

where ∇u is constant per triangle and given by $\nabla u = (\sum_{j=1}^{3} u_j \vec{n}_j)/2S_T$. It is straightforward to show that this discretiation is identical with that produced by the Galerkin method. Indeed, the finite element approximation of $\nu\Delta u$ at node i is obtained by multiplying by the test function ω_i with compact support Ω_i and integrating by parts. One has

$$\iint_{\Omega_i} \omega_i \nu \Delta u \, d\Omega = \underbrace{\oint_{\partial\Omega_i} \omega_i \nu \nabla u \cdot d\vec{n}_{ext}}_{=0} - \iint_{\Omega_i} \nabla\omega_i \cdot \nu \nabla u \, d\Omega$$

$$= -\sum_{T\in\Omega_i} \iint_T \frac{\vec{n}_i}{2S_T} \cdot \nu \nabla u \, d\Omega = -\sum_{T\in\Omega_i} \frac{\nu}{2} \nabla u \cdot \vec{n}_i.$$

The update scheme for the convection–diffusion equation can then be written as

$$u_i^{n+1} = u_i^n - \frac{\Delta t}{S_i} \sum_{T, T\in\Omega_i} \left(\beta_i^T (S_T \vec{\lambda} \cdot \nabla u) + \frac{\nu}{2} \nabla u \cdot \vec{n}_i \right). \tag{14}$$

Note that for a given triangle T the contributions to the three vertices due to the Galerkin formulation of the diffusion term cancel out:

$$\frac{\nu}{2} \nabla u \cdot (\vec{n}_i + \vec{n}_j + \vec{n}_k) = 0.$$

For pure diffusion the scheme is positive provided that the grid satisfies certain regularity conditions (e.g. Delaunay triangulation[10]) and the following time step restriction is made:

$$\Delta t \leqslant \frac{4S_i}{\nu \sum_{T, T\in\Omega_i} \| \vec{n}_i \|^2 / S_T}. \tag{15}$$

Indeed, writing out the scheme explicitly in terms of the values of u in the surrounding nodes, we get

$$u_i^{n+1} = u_i^n - \frac{\Delta t}{S_i} \frac{\nu}{2} \sum_{T, T\in\Omega_i} \frac{1}{2S_T} \sum_{j=1}^{3} u_j^n \vec{n}_j \cdot \vec{n}_i = \sum_j c_j u_j^n. \tag{16}$$

Thus the coefficient of u_i^n is given by

$$c_i = 1 - \frac{\Delta t}{S_i} \frac{\nu}{2} \sum_{T, T\in\Omega_i} \frac{1}{2S_T} \| \vec{n}_i \|^2, \tag{17}$$

which is positive under the condition (15). The other coefficients $c_{j,j\neq i}$ are positive for geometric reasons.

3.2. *Residual-based approach*

A residual-based discretization for the convection–diffusion equation (1) is now discussed. The cell residual ϕ^T consists of the convection term ϕ^C, which is evaluated as usual by assuming linear variations in u over the cell, and the balance of the viscous fluxes ϕ^D given by

$$\phi^D = -\int\int_T \nu \Delta u \, d\Omega = -\oint_{\partial T} \nu \nabla u \cdot \, d\vec{n}_{ext}. \tag{18}$$

Assuming a constant gradient over T leads to a vanishing viscous residual ϕ^D. Therefore a higher-order reconstruction and an extension of the computational stencil are necessary to recover ∇u on the boundary ∂T. Two alternatives are considered.

(a) *Nodal gradients.* The gradients are recovered at the nodes by an area-weighted average over Ω_i:

$$\nabla u_i = \frac{\sum_{T \in \Omega_i} S_T \nabla u_T}{\sum_{T \in \Omega_i} S_T}. \tag{19}$$

Once the value of ∇u is known at each vertex, ϕ^D can be evaluated using the trapezoidal rule (piecewise linear interpolation) as

$$\phi^D = -\frac{\nu}{2} \sum_{i=1}^{3} \nabla u_i \cdot \vec{n}_i, \tag{20}$$

where $\vec{n}_i$ are the inner normals to the triangle introduced in Section 2.

(b) *Edge-based gradients.* The gradients are recovered at the midpoint of each edge:*

$$\nabla u_e = \frac{1}{2}(\nabla u_{T_1} + \nabla u_{T_2}), \tag{21}$$

where T_1 and T_2 are the cells on either side of edge e. The diffusion term is then evaluated as

$$\phi^D = \nu \sum_{e=1}^{3} \nabla u_e \cdot \vec{n}_i, \tag{22}$$

where i is the node opposite edge e, as shown in Figure 4.

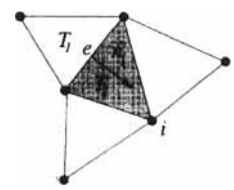

Figure 4. Evaluation of ϕ^D using edge-based gradients

* A possibly more accurate formula would be $\nabla u_e = (S_{T_2} \nabla u_{T_1} + S_{T_1} \nabla u_T)/(S_{T_1} + S_{T_2})$, which reduces to (21) for regular grids such as considered in the present numerical investigations (Section 4).

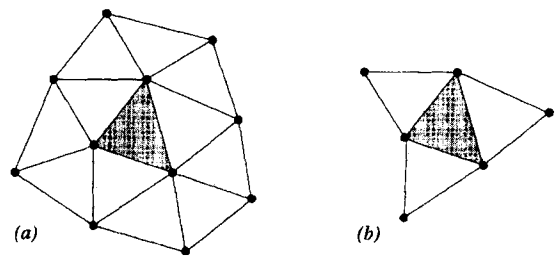

Figure 5. Stencils used to estimate (a) nodal gradients and (b) mid-edge gradients

Once ϕ^D has been evaluated by either (20) or (22), it can be distributed along with ϕ^C using the residual distribution schemes described in Section 2, giving the update scheme

$$u_i^{n+1} = u_i^n - \frac{\Delta t}{S_i} \sum_T \beta_i^T (\phi_C + \phi^D). \tag{23}$$

Compared with the Galerkin method described in the previous section, this approach has the disadvantage of requiring a larger stencil, as shown in Figure 5. In addition, it does not provide a positive discretization in the limit of pure diffusion, as can be easily shown by considering a uniform flow aligned with one grid line direction of a regular grid, for which the distribution scheme is a single target for all triangles.

4. NUMERICAL RESULTS

4.1. Shear layer/flat plate interaction

The interaction of a shear layer with a flat plate upon which develops a boundary layer is computed. A uniform triangulation of the domain $(x, y) \in [0, 1]^2$ is used, with equal spacing in both directions, $\Delta x = \Delta y = \frac{1}{60}$. The convection speed vector $\vec{\lambda}$ is uniform, equal to $2\vec{e}_x + \vec{e}_y$, where $\vec{e}_x$ and e_y indicate unit vectors in the directions x and y respectively. The diffusion coefficient ν is taken equal to 10^{-3}, corresponding to a cell Peclet number $Pe \approx 37$. The solution is specified on all the boundaries as

$$u = 0 \quad \begin{cases} \text{on } x = 1 \text{ and } 0 \leqslant y \leqslant 1, \\ \text{on } y = 0 \text{ and } 0 \leqslant x \leqslant 1, \end{cases}$$

$$u = 1 \quad \begin{cases} \text{on } x = 0 \text{ and } 0 \leqslant y \leqslant 1, \\ \text{on } y = 1 \text{ and } 0 \leqslant x \leqslant 1. \end{cases}$$

The two approaches described previously are compared: the upwind/central discretization and the residual-based discretization. For the latter the reconstruction of the viscous residual is done using either nodal gradients or edge-based gradients. The complete residual is then upwinded using the MinMod scheme. The following computations are performed:

(a) mixed upwind/central: PSI/Galerkin
(b) residual MinMod^a (with nodal gradients)
(c) residual MinMod^b (with edge-based gradients)
(d) residual MinMod^a (with nodal gradients) on a fine mesh 221×221.

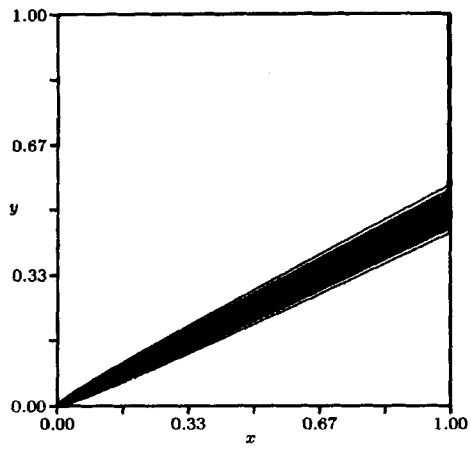

Figure 6. Shear layer/flat plate interaction: reference solution

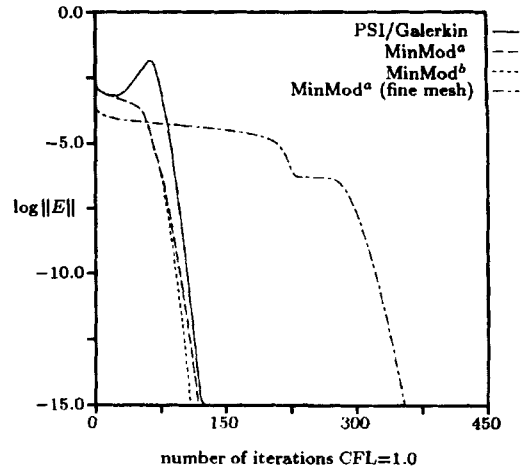

Figure 7. Shear layer/flat plate interaction: convergence histories

The fine mesh solution is considered as a reference solution and is plotted in Figure 6. The convergence histories corresponding to forward Euler time stepping and $CFL = 1{\cdot}0$ are plotted in Figure 7 and show the same trends, although it must be noted that at this value of the Courant number the mixed upwind/central scheme is at the limit of stability. A cut of the solutions across the shear layer (at $x = 0{\cdot}8$) is made and shown in Figure 8. The solutions on the 61×61 mesh nearly all coincide and are all quite far from the reference solution, suggesting that the mesh is not fine enough to resolve the shear layer. All the solutions are perfectly monotone owing to the use of positive convection schemes (PSI, MinMod). A detailed cut shown in Figure 9 indicates that the residual-based approach is actually more accurate than the classical upwind/central approach, with a slight advantage to the formulation using edge-based gradients. However, the advantage in terms of accuracy is not decisive.

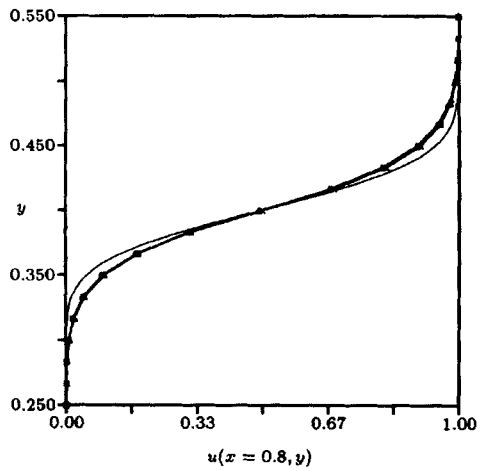

Figure 8. Shear layer/flat plate interaction: cut at $x = 0{\cdot}8$

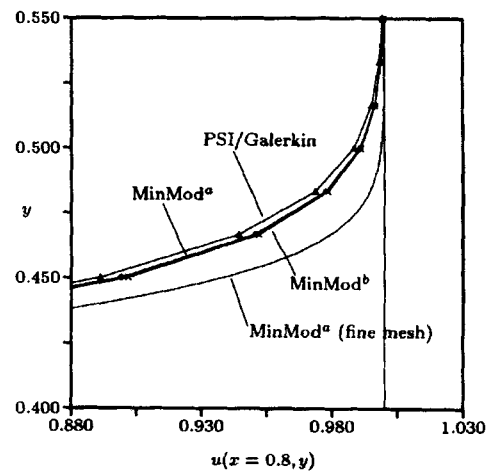

Figure 9. Shear layer/plate interaction: cut at $x = 0{\cdot}8$, close-up view

4.2. *The Smith and Hutton problem*

This classical test case was proposed in 1981 during a workshop on 'Numerical Representation of Advection'. A large number of methods were compared and the results reported by Smith and Hutton.[11] The problem is characterized by a fairly complicated streamline pattern and steep gradients in the quantity being convected. Unlike in the previous test case, no boundary layers are present in the flow. The velocity field is specified analytically as

$$\vec{\lambda}(x, y) = 2y(1 - x^2)\vec{e}_x - 2x(1 - y^2)\vec{e}_y$$

on the domain $(x, y) \in [-1, 1] \times [0, 1]$ and is depicted in Figure 10. On the outlet boundary ($y = 0$ and $0 < x < 1$), $\partial u/\partial y = 0$ is imposed, either weakly by leaving u unspecified or strongly in the case where ∇u is reconstructed at the nodes. The solution is imposed on all other boundaries as

$$u(x, 0) = 1 + \tanh[(2x + 1)\alpha] \quad \text{on } y = 0 \text{ and } -1 \leqslant x \leqslant 0,$$

$$u(x, y) = 1 - \tanh \alpha \begin{cases} \text{on } x = -1 \text{ and } 0 \leqslant y \leqslant 1, \\ \text{on } y - 1 \text{ and } -1 \leqslant x \leqslant 1, \\ \text{on } x = 1 \text{ and } 0 \leqslant y \leqslant 1, \end{cases}$$

where α is given the value 10. A structured grid with 41 × 21 points was chosen, since this seems to have been the most popular choice among the contributions compared in Reference 11. Three cases were selected from that workshop, namely $\nu = 10^{-1}$, 10^{-3} and 10^{-6}, corresponding respectively to

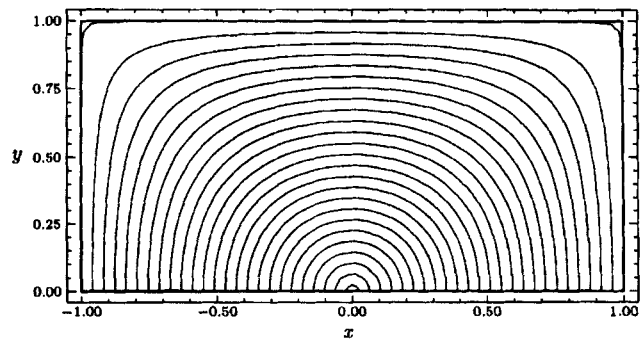

Figure 10. Smith and Hutton problem: streamline pattern

Table II. Smith and Hutton problem: summary of minimum/maximum solution values

Scheme				
Convection	Diffusion	$Pe = 1, \nu = 10^{-1}$	$Pe = 100, \nu = 10^{-3}$	$Pe = 10^5, \nu = 10^{-6}$
Galerkin	Galerkin	0·0000, 2·0000	−0·0014, 2·0000	Not converged
SUPG	Galerkin	0·0000, 2·0000	−0·0002, 2·0000	−0·0101, 2·0116
LDA	Galerkin	0·0000, 2·0000	−0·0006, 2·0000	−0·0249, 2·0101
PSI	Galerkin	0·0000, 2·0000	0·0000, 2·0000	0·0000, 2·0000
SUPG + AV	Galerkin	0·0000, 2·0000	0·0000, 2·0000	−0·0001, 2·0002
MinMod[a]	Residual	0·0000, 2·0000	0·0000, 2·0000	0·0000, 2·0000
LDA[a]	Residual	0·0000, 2·0000	−0·0028, 2·0000	−0·0248, 2·0098

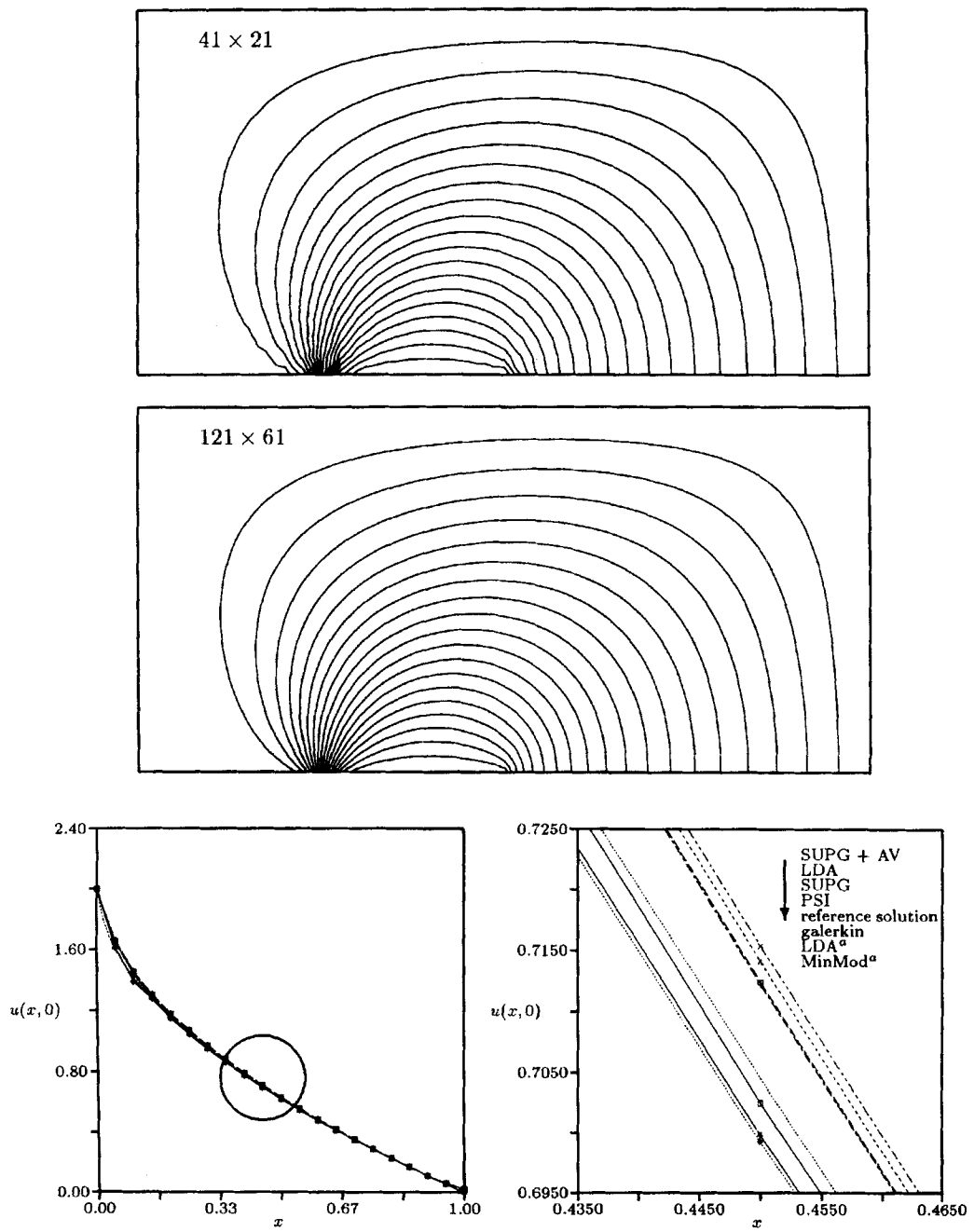

Figure 11. Smith and Hutton problem, $\nu = 10^{-1}$: (from top to bottom) PSI/Galerkin solution on 41 × 21 grid, reference solution on 121 × 61 grid and cut along outlet boundary with close-up of circled region

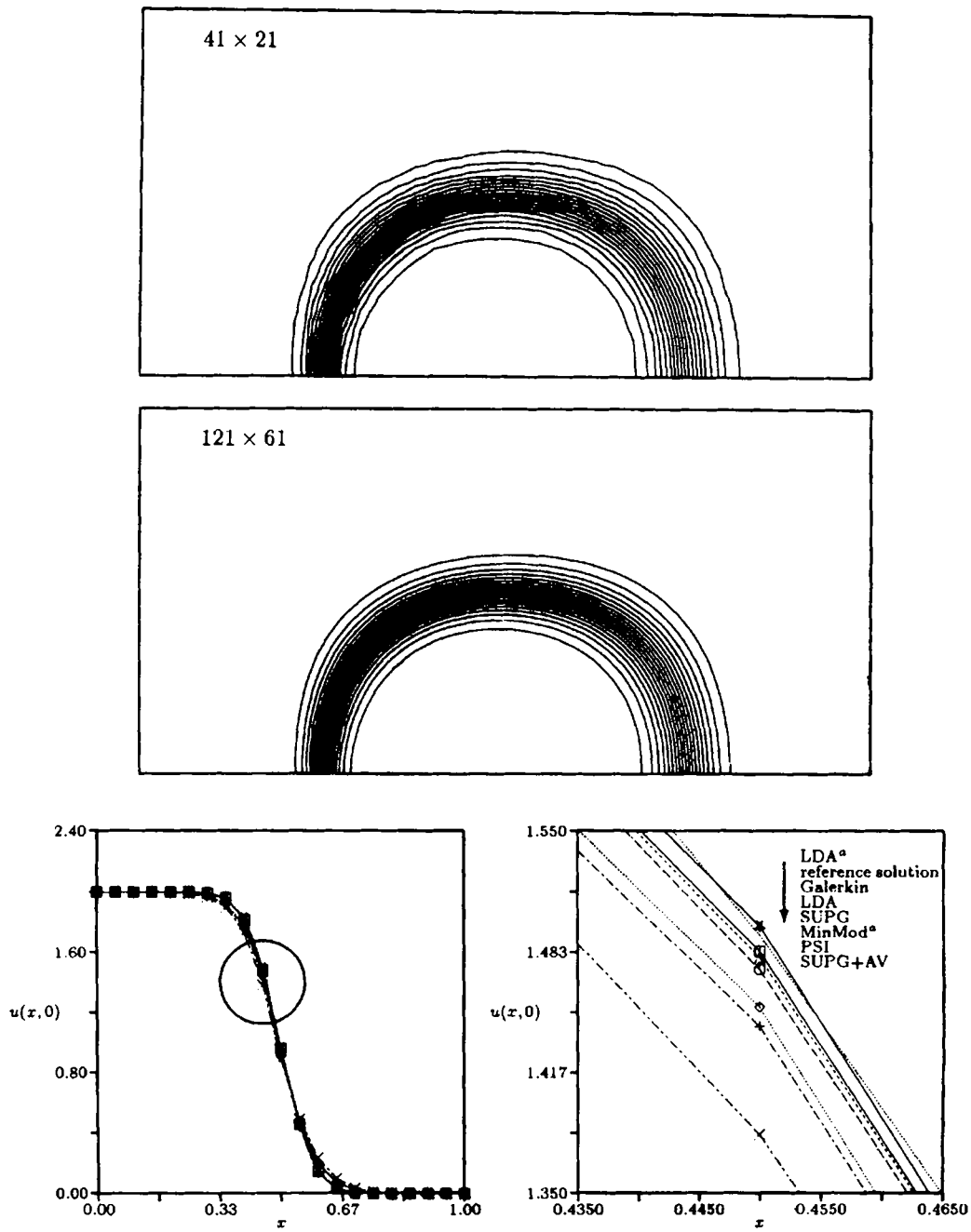

Figure 12. Smith and Hutton problem, $\nu = 10^{-3}$: (from top to bottom) PSI/Galerkin solution on 41 × 21 grid, reference solution on 121 × 61 grid and cut along outlet boundary with close-up of circled region

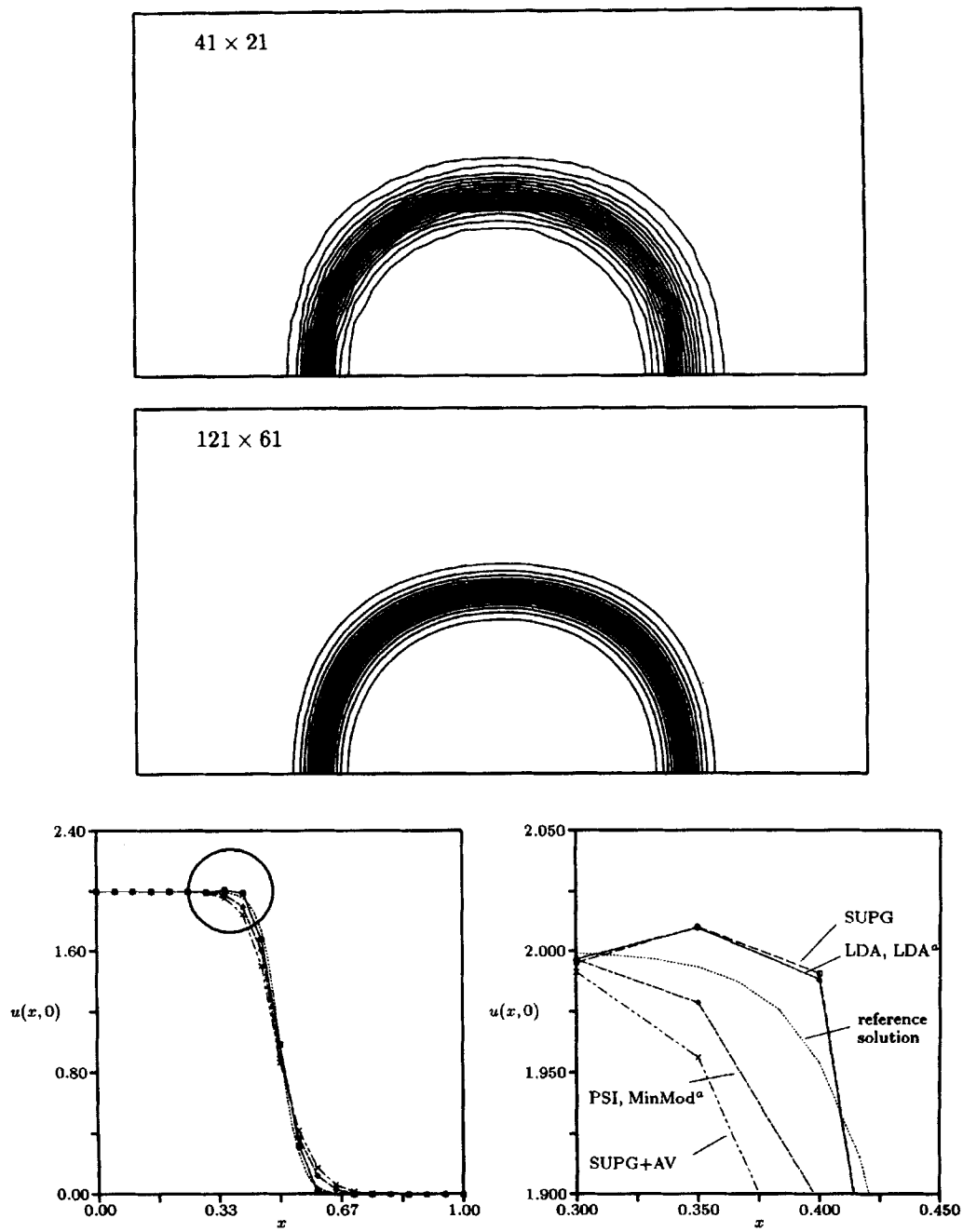

Figure 13. Smith and Hutton problem, $\nu = 10^{-6}$: (from top to bottom) PSI/Galerkin solution on 41 × 21 grid, reference solution on 121 × 61 grid and cut along outlet boundary with close-up of circled region

$Pe = 1$, 100 and 10^5. The first case is diffusion-dominated whereas the latter is convection-dominated. In the absence of an exact analytical solution to this problem, a fine grid solution (121×61) is selected in each case as the reference solution.

The results are summarized in Table II, in which the range $[u_{\min}, u_{\max}]$ is given in each case to indicate the presence or absence of oscillations. The following observations can be made.

$Pe = 1$. This case is dominated by diffusion. Convection and its discretization play almost no part. It is not surprising therefore that the solutions obtained using various convection schemes for the inviscid term and central differencing (Galerkin) for the viscous term fall neatly onto one another; see cut in Figure 11. The Galerkin method, corresponding to distribution coefficients $\beta_i^{\text{Gal}} = \frac{1}{3}$ can even be used for the convective term without affecting the stability or monotonicity of the solution. The residual-based approach (MinMod^a and LDA^a) leads to slightly more accurate solutions than the mixed upwind/central discretization, especially near the origin ($0 < x < 0{\cdot}1$). This shows that the method can also be applied to very viscous flows.

$Pe = 100$. This case is dominated by convection, but diffusion effects are important enough to damp oscillations that appear when a non-positive convection scheme is used. The solutions obtained using the residual-based approach are as accurate, if not more so, than the solutions obtained with the upwind/central approach, as observed from the close-up view of the cut shown in Figure 12.

$Pe = 10^5$. This case is almost pure convection and the diffusion present in the solution is essentially due to the false dissipation of the convection schemes. The Galerkin method did not converge and solutions obtained using non-positive convection schemes (LDA, SUPG) are oscillatory; see Figure 13. For this value of the Peclet number the diffusion is so small that no difference can be observed between the two approaches PSI/Galerkin and MinMod^a or LDA/Galerkin and LDA^a.

5. CONCLUSIONS

Two approaches for discretizing the convection–diffusion equation have been compared. The first is based on the use of a multidimensional residual distribution scheme (PSI, LDA, SUPG, etc.) for the discretization of the convective term and on the use of the Galerkin discretization for the viscous term. The second approach is more original and more expensive than the first and consists of applying upwind residual distribution schemes to both the inviscid flux balance and the viscous flux balance, evaluated by reconstructing nodal gradients or edge-based gradients. This approach is slightly more accurate than the classical approach even for very low Peclet number flows, but the improvement on the whole does not justify the additional cost and extension of the stencil.

REFERENCES

1. K. W. Morton, P. I. Crumpton and J. A. Mackenzie, 'Cell vertex methods for inviscid and viscous flows', *J. Comput. Fluids*, **22**, 91–102 (1993).
2. H. Deconinck, R. Struijs, G. Bourgois and P. L. Roe, 'Compact advection schemes on unstructured grids', in *VKI LS 1993-04, 1993.*
3. G. T. Tomaich and P. L. Roe, 'Compact schemes for advection–diffusion problems on unstructured grids', *Proc. 23rd Ann. Modeling and Simulating Conf.*, 1992.
4. J. Boxho and G. Degrez, 'Numerical solution of advection–diffusion equation on unstructured meshes using advection schemes', *Tech. Rep. PR-1993-06*, Von Karman Institute, 1993.
5. J. -C. Carette, H. Deconinck, H. Paillère and P. L. Roe, 'Multidimensional upwinding: its relation to finite elements', *numerical methods fluids*, **20**, 935–955 (1995).

6. H. Paillère, H. Deconinck and A. Bonfiglioli, 'A linearity-preserving wave-model for the solution of the Euler equations on unstructured meshes', *Proc. 2nd Eur. CFD Conf.*, Wiley, Chichester, 1994, pp. 309–316.
7. D. Sidilkover and P. L. Roe, 'Unification of some advection schems in two dimensions', *Tech. Rep. 95-10*, ICASE, 1995.
8. H. Paillère, Multidimensional upwind residual distribution schemes for the Euler and Navier–Stokes equations on unstructured grids', *Ph.D. Thesis*, Université Libre de Bruxelles, 1995.
9. C. Johnson, A Szepessy and P. Hansbo, 'On the convergence of shock-capturing streamline diffusion finite element methods for hyperbolic conservations laws', *Math. Comput.*, **54**, 107–129 (1990).
10. T. J. Barth, 'On unstructured grids and solvers', in *VKI LS 1990-04*, 1990.
11. R. M. Smith and A. G. Hutton, 'The numerical treatment of advection: a performance comparison of current methods', *Numer. Heat Transfer*, **5**, 439–461 (1982).